Engineering Preformed Cobalt-Doped Platinum Nanocatalysts For Ultraselective Hydrogenation

Shik Chi Tsang,[†,*] Nick Cailuo,[†] William Oduro,[†] Adam T. S. Kong,[†] L. Clifton,[†] K. M. Kerry Yu,[†] Benedicte Thiebaut,[‡] James Cookson,[‡] and Peter Bishop[‡]

[†]Wolfson Catalysis Centre, Inorganic Chemistry, University of Oxford, Oxford, OX1 3QR, U.K., and [‡]Johnson Matthey Technology Centre, Sonning Common, Reading RG4 9NH, U.K.

ABSTRACT Bimetallic heterostructures are used as industrial catalysts for many important transformations. However, conventional catalysts are primarily prepared in cost-effective manners without much appreciation in metal size control and metal—metal interaction. By employing recent nanotechnology, Pt nanocrystals with tailored sizes can be decorated with Co atoms in a controlled manner in colloid solution as preformed nanocatalysts before they are applied on support materials. Thus, we show that the terminal C═O hydrogenation can be achieved in high activity, while the undesirable hydrogenation of the C═C group can be totally suppressed in the selective hydrogenation of α,β-unsaturated aldehydes to unsaturated alcohols, when Co decorated Pt nanocrystals within a critical size range are used. This is achieved through blockage of unselective low coordination sites and the optimization in electronic influence of the Pt nanoparticle of appropriate size by the Co decoration. This work clearly demonstrates the advantage in engineering preformed nanoparticles *via* a bottom-up construction and illustrates that this route of catalyst design may lead to improved catalytic processes.

KEYWORDS: size effect · catalytically active site · bimetallic · hydrogenation · electronic effect · site blocking

It is long known that specific sites are responsible for different molecular reactions taking place on the surface of a catalyst. By understanding the molecular interrelations, one may be in a position to manipulate the catalyst's selectivity on an atomic basis. It is noted that achieving 100% selectivities is one of the key goals for present and future research in the field of catalysis. Thus, in order to enhance the reaction selectivity, the nature of the surface sites (which are size and shape dependent) must be carefully defined and controlled. The recent tailoring of metal nanostructures with controlled size and shape by lithographic techniques[1] and by nanochemistry synthetic skills[2] provides interesting approaches, but little investigation has been undertaken using bimetallic nanostructures. This would be particularly advantageous, since in selective catalytic hydrogenations bimetallic catalysts have proven to exhibit superior performance as compared to their monometallic counterparts.[3]

In the fields of flavor and fragrance chemistry and pharmaceuticals, the selective hydrogenation of unsaturated carbonyl intermediates (such as α,β-unsaturated aldehydes) to their corresponding unsaturated alcohols is a vitally important reaction. Although the reduction can be achieved using stoichiometric amounts of reducing agents, such as metal hydrides, there are increasing stringent requirements on modern industrial processes regarding atom efficiency, energy consumption, waste product disposal, and sustainability. Consequently, a new heterogeneous catalysis process achieving 100% selectivity toward desirable hydrogenated products without any side-product formation would be preferred to avoid any loss of energy efficiency and waste post-treatment. Solid supported bimetallic catalysts have been extensively investigated in recent years,[3−6] and these appear to be the promising candidates for the hydrogenation of α,β-unsaturated aldehydes to the corresponding unsaturated alcohols. The addition of a second metal to either supported Pt or Pd metals (that are synthesized *via* conventional routes, that is, coprecipitation, coimpregnation, surface organometallic reactions, *etc.*) results in a higher selectivity toward the unsaturated alcohol, which is generally attributed to the active interface created. Thus, a wide variety of catalysts with two or more metallic components, on different support materials, have been studied. It has been proposed that the second metal provides geometric and electronic modifications to the surface.[3−6] However, the traditional approaches for these catalyst preparations do not produce well-defined samples (with problems including uncontrolled metal/

See the accompanying Perspective by F. C. Meunier on p 2441.

*Address correspondence to edman.tsang@chem.ox.ac.uk.

Received for review June 25, 2008 and accepted October 14, 2008.

Published online November 5, 2008.
10.1021/nn800400u CCC: $40.75

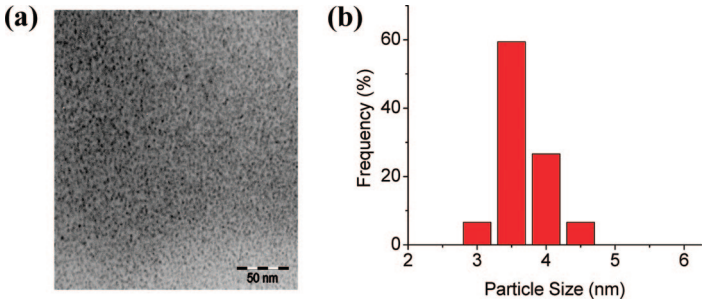

Figure 1. (a) A TEM showing 3.3 nm Pt nanocrystals made from chemical reduction at elevated temperature; (b) a sharp particle-size distribution derived from TEM micrograph, illustrating that most Pt particles are within 3.5 ± 0.5 nm.

metal morphology and interface, poor control in particle size, support effects). A poor understanding of these parameters hinders future development. As a result, further intensive efforts in exploring new formulations of supported metallic catalysts, prepared using traditional synthesis, may not be justified in solving this intrinsic problem unless some fundamental understanding on the mechanism can first be obtained. It is noted that no catalyst has previously been identified that produces α,β-unsaturated alcohols as exclusive products.

In this work, we exploited nanochemistry preparative skills; the use of a modified colloid preparative technique,[2,7−10] for the syntheses of unsupported Pt nanoparticles and the Co atoms decorated Pt nanoparticles of controlled and well-defined sizes. The latter was achieved *via* a sequential chemical reduction in the presence of the preformed Pt nanoparticles as seeds (see Methods). Subsequently, we investigated the size effects of these unsupported, unmodified-Pt and codecorated-Pt nanoparticles for the hydrogenation of α,β-unsaturated aldehydes (such as cinnamaldehyde and citral) to the corresponding alcohols.

RESULTS AND DISCUSSION

The resulting Pt nanoparticles displayed uniformed Pt particle distributions; a typical TEM micrograph (Figure 1a) shows small, nearly monodispersed Pt particles (confirmed by EDX) of around 3.3 nm (±0.5 nm) (Figure 1b). This diameter agrees well with our evaluation from the line broadening of Pt⟨111⟩ XRD peak using the Scherrer equation. Under a careful examination of the TEM micrograph, all of the particles appear to be spherical or slightly faceted nanocrystals with the Pt (111) and (200) lattice fringes clearly visible from the imaging (Figure 2). Varying the concentration of the stabilizers enabled the size of nanocrystals to be controlled, while maintaining their similar morphology and narrow size distribution. Therefore, this process can produce nearly monodispersed nanocrystals of well-defined sizes. These are listed in Table 1 together with their associated selectivity toward the reduction of cinnamaldehyde. For example, the 2.8 nm particles gave

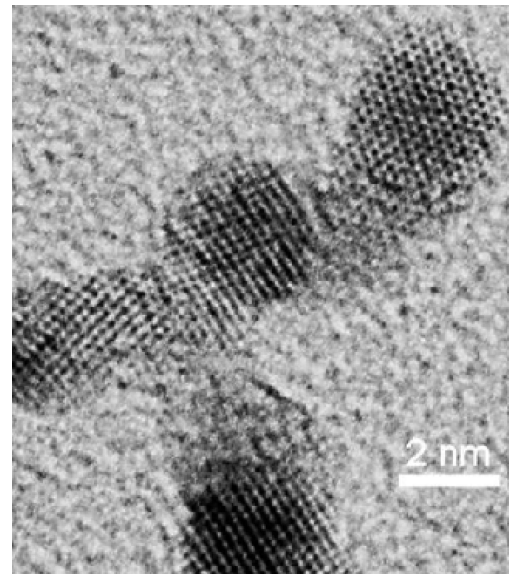

Figure 2. High resolution TEM showing typical 3.3 nm Pt nanocrystals (2.27 and 1.96 Å lattice fringes correspond to Pt (111) and (200) planes, respectively).

24.8% selectivity, while the 14.4 nm particles showed 85.6%. This suggests that this reaction is structure sensitive, according to Boudart's classification.[4] It has been demonstrated that different surface metal sites (*i.e.*, corners, steps, and terraces) on the Pt crystal give different selectivities for this hydrogenation reaction. The proportion of sites available can be greatly varied by changing the crystal size: with selectivity being inversely dependent on size of crystal.[3−6] This result is therefore consistent with earlier studies of gas-phase hydrogenation of α,β-unsaturated aldehydes on well-defined single crystal surfaces, which showed the importance of specific modes of adsorption on metal crystal faces and structure of the substrate molecule on the overall selectivity. According to theoretical calculations from Delbecq *et al.*,[11] flat surfaces, such as Pt(111), adsorb the α,β-unsaturated aldehyde in a terminal di-σ_{co} mode. This leads to the preferential termi-

TABLE 1. Nanocrystal Particle Size and Selectivity toward Cinnamyl Alcohol[a]

Particle size (nm)	cinnamyl alcohol selectivity %
2.8	24.3
3.1	30.2
3.3	44.6
4.8	49.1
6.0	80.8
14.4	85.6
24.8 (sintered)	85.3

[a]Average particle size was deduced by TEM; 37 mg of unsupported Pt nanocrystals, 5 mL of 12.5% vol/vol cinnamaldehyde in IPA, 20 bar H_2, 100 °C for 2 h were placed in 25 mL stainless steel autoclave. The liquid sample was analyzed with GC-FID and GC−MS to identify and quantify all products, which showed a total consumption of cinnamaldehyde under the reaction conditions. Only two main products, the unsaturated alcohol (cinnamyl alcohol) and the saturated aldehyde (hydrocinnamaldehyde) were obtained with only traces of phenylpropanol detected.

nal aldehyde being reduced to unsaturated alcohol. In contrast, low coordination sites (such as corners, kinks, adatoms, and defective sites) favor π interactions with C═C, which account for unselective products. The fraction of low coordination sites decreases with the increase in the size of Pt crystals,[12] thus accounting for the corresponding increase in the selectivity to the unsaturated alcohol. With our accurate control in Pt crystallite size, this present work clearly underpins the size effect on selectivity of this hydrogenation, which can be separated from the effects of support and chemical promotion. However, it is interesting to observe that the selectivity to unsaturated alcohol *converges to around 85%*, despite further enhancement in particle size. Detailed analysis also reveals that the selectivity depends on the coverage of the substrate molecule (with high concentrations of the substrate favoring the terminal aldehyde hydrogenation, due to steric effects that inhibit the hydrogenation of the C═C bond of cinnamaldehyde[6]). These results gave two implications: First, the nature of adsorption mode that dictates the chemoselectivity is dynamic, depending on both the surface coverage and crystal planes. Therefore using larger unmodified Pt crystals may not further raise the selectivity to 100%. Second, the use of larger crystallites is commercially less attractive regarding atom efficiency (maximizing productivity per gram of catalyst used). The effect of atomic decorations on these Pt nanocrystals was then studied.

Modification of Pt by adding a second metal for the same reaction over conventional catalysts has previously been extensively studied. It has been reported that significant improvements in the selectivity can be achieved, but this selectivity rarely exceeded 90%. For example, one report described the preparation of a platinum−cobalt bimetallic catalyst on carbon support, prepared by a coimpregnation method. This displayed a selectivity of 90% to cinnamyl alcohol, which is among the highest value reported in the literature.[3] A cobalt−boron catalyst has also been shown to exhibit high activity and selectivity (87.6%), for the same reaction.[13] Following this precedent, the Pt nanocrystals prepared by our method were decorated with Co and other metals.

Co decoration of Pt nanocrystals was achieved by the reduction of $Co(acac)_2$ at elevated temperatures, in the presence of the preformed 4.8 nm Pt nanoparticles. Table 2 displays the dramatic effect that this decoration bestows upon the reaction selectivity. The selectivity to the unsaturated alcohol initially increases with increasing content of the Co precursor added to the reaction mixture. After the addition of approximately one molar equivalent of cobalt the selectivity levels off at ≥99.8% selectivity, with a complete conversion of the substrate. TEM revealed that there was no apparent change in the Pt morphology, but both EDX and ICP analyses showed a small level of Co deposited onto

TABLE 2. Co Decoration on Pt Nanoparticles (4.8 nm)[a]

molar ratio Co/Pt recipe (EDX Co/Pt ratio of solid product)	% cinnamaldehyde conversion	% selectivity to cinnamyl alcohol
0 (0)	18.82	41.4
0.24 (0.17)	58.38	61.2
0.49 (0.18)	81.77	73.6
0.98 (0.18)	91.06	99.6
1.47 (0.18)	90.83	99.1
3.91 (n.d)	76.40	98.1

[a]Initially, 4.8 nm Pt seeds were prepared using a solution mixture of platinum acetyl acetonate (99.99%, Aldrich, 0.30 g), 1,2-hexadecanediol (90%, Aldrich, 0.20 g), 120 μL of oleic acid, (99+%, Aldrich), and 120 μL of oleylamine (98%, Aldrich) in 10 mL of octylether (99%, Aldrich) refluxed at 250 °C for 40 min in a three-necked round-bottom flask in an inert environment. This was followed by adding cobalt acetyl acetonate, $Co(acac)_2$, (min 97%, Merck) with the quantity shown in the table relevant to Pt in 5.0 mL of octylether, 64 μL of oleic acid, and 1,2-hexadecanediol (90%, Aldrich, 0.50 g) at room temp before the mixture was heated to 250 °C for 20 min.

the Pt (leveling off at a 0.18 Co/Pt ratio), despite a large excess of Co precursor added to the reaction mixture (it is attributed to the fact that only the low coordinated Pt sites can selectively take up Co atoms from solution). Under the same conditions, we demonstrated that Co^{2+} could not be reduced without the presence of Pt seeds. This implies that catalytic deposition onto Pt nanocrystal was occurring, by this technique.

It is noteworthy that using Co decoration gave the optimum selectivity in cinnamaldehyde hydrogenation. The preformed 4.8 nm Pt nanoparticles were also decorated by the addition of a range of other second metals, including the first row transition elements. While the addition of Mn and Fe gave rise to increased selectivities (not shown) in comparison to the undecorated Pt nanoparticles, overall lower selectivities were observed, with Co appearing at the optimum point of a volcano plot.

Our remarkable result, with virtually 100% selectivity at the complete cinnmaldehyde conversion, is very intriguing and interesting. Similarly, remarkably high selectivities in the hydrogenation of more challenging α,β-unsaturated aldehydes to corresponding unsaturated alcohol such as citral (>96% selectivity to the isomers nerol and geraniol, not shown) at decent conversions is also found; thus highlighting the versatility of the catalyst. As far as we are aware, these selectivities are the highest, among all those reported in the literature, for this reaction using Pt-based catalysts. It is therefore interesting to explore further the Co atoms decorated Pt synthesized by our method.

Figure 3 reveals a very interesting size effect of Co atom-decorated Pt nanocrystals (synthesized using an equimolar Co/Pt ratio), which has not previously been observed. The figure shows that crystal sizes smaller than 6 nm were found to give >99.6% while larger crystal size such as 22.5 nm only resulted in selectivities of ~85%. It is interesting to note that the latter particle

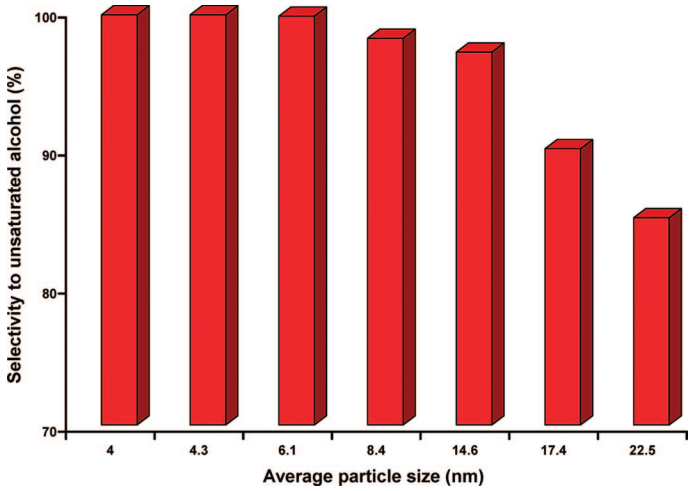

Figure 3. Selectivity to cinnamyl alcohol (at virtually 100% conversion) dependent on size of Co-decorated Pt nanocrystals.

size yielded the same selectivity as the large unmodified Pt crystals (Table 1).

From this work, several fundamental questions arise: Why is the selectivity dependent on Pt size, but inversely dependent on Co-decorated Pt size? What is the role of Co in determining the remarkably high selectivities? If it has more than one function, then how can we differentiate its effects? Why do Co-decorated Pt nanocrystals, prepared by our nanochemical techniques, display significantly superior selectivities compared to those catalysts prepared by conventional techniques?

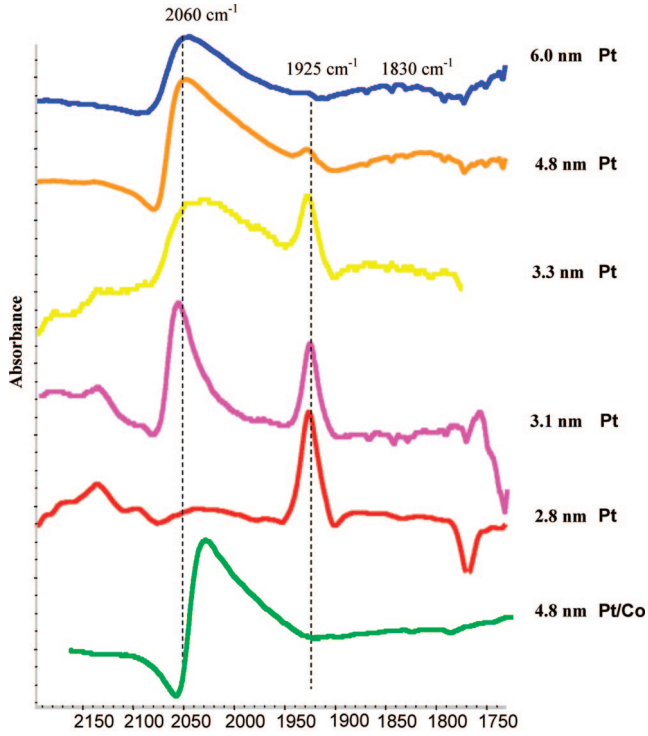

Figure 4. ATR-FTIR spectra of CO adsorbed at room temperature (a flowing stream of 1 atm CO gas using golden gate reactor) on Pt nanocrystals of different sizes and Co-decorated Pt nanocrystal.

To address these questions, the Pt surface of the catalyst was carefully examined using a probe molecule; CO was adsorbed onto the Pt surface and this was subsequently examined by infrared spectroscopy. Figure 4 shows CO adsorption spectra of different-sized Pt nanocrystals, using a surface sensitive ATR-IR technique at 1 atm under a flowing stream of CO. The IR spectra obtained gave rise to at least two distinctive $\upsilon_{c=o}$ bands; the first, appearing between 2090 and 2040 cm^{-1} (peaked at 2060 cm^{-1}) is attributed to linearly adsorbed CO on one Pt atom, and the second, at around 1860−1780 cm^{-1} (a broad peak at 1830 cm^{-1}), is assigned to CO bridging on two or more Pt atoms.[14,15] This assignment was corroborated by results obtained on single crystal planes and supported metal particles. This suggests that platinum adsorbs CO predominantly in a linear manner, with a low occupancy of bridged sites at high CO coverage.[14] However, when the Pt nanocrystals become smaller, a new band arises at approximately 1925 cm^{-1}, and this peak is more prevalent with decreasing particle size. This band is characteristic of the stretching mode of multi-CO, in which more than one CO molecules are bound to a low coordination Pt atom, and is typically found in spectra of molecular Pt carbonyl complexes.[16] It is noted that finely dispersed supported noble metals can also give rise to multicarbonyl species, particular the dicarbonyl on lower coordination metal atoms (such as corners, steps, adatoms, or defective sites).[17] This can therefore explain our observation of the increasing intensity of this peak in smaller particles. However, one important point that should be noted is that the predominance of this multicarbonyl species at 2.8 nm in our case, as compared with the principal linear mode on supported Pt nanoparticles, is rather unusual and surprising. On the other hand, the surfaces of small Pt nanocrystals prepared under the mild conditions used in colloidal metal preparations have not been exposed to conditions that would cause annealing to the most stable surface structure. As a result of this they differ from most conventional prepared supported platinum particles in heterogeneous catalysts which are often subjected to thermal treatment before use. We attribute this to the fact that because the nanochemistry synthesis used mild reaction conditions, the smaller nanocrystals contain higher proportions of defected and low-coordinated metal surfaces, despite the exceptional geometrically regular crystalline Pt nanocrystals, as observed by the TEM. Thus, the increasing occupancy of these low coordination surface sites at smaller size accounts for the decrease in reaction selectivity. In contrast, larger-sized Pt particles with an increasing proportion of flat surfaces contain a relatively lower abundance of these defective sites, which would enhance the reaction selectivity. However, it is interesting that the selectivity converges at a maximum of 85% for large Pt crystals. It clearly appears that the dynamic adsorption of the un-

saturated aldehyde on the remaining terrace sites for the large crystals cannot further enhance the reaction selectivity, without the promotion of a second metal. On the other hand, it is very remarkable to find that Co atoms preferentially segregate at the sites of low coordination on the surface of the Pt crystal. This can totally suppress the formation of multicarbonyl peak in the CO adsorbed ATR-IR spectra in all the Co-containing samples, despite their low surface coverage (see EDX, ICP, XPS data).

Electrochemical techniques have previously been used to elucidate their structures of Pt surfaces.[18] Cyclic voltammograms (CVs) indicated the disappearances of Pt{111} × {111} and Pt{100} × {111} steps (distinctive features in CVs of Pt/graphite that correspond with single crystal data[19]) upon the decoration of Co atoms. This site blocking (coverage) on platinum nanoparticles by Co atoms was also confirmed using pulse CO chemisorption (CV and chemisorption data not shown). Thus, the preferential site blocking by Co atoms reinforces our earlier postulation of catalytic deposition on low coordination, and highly reactive sites, and the subsequent reduction of Co^{2+} in the presence of Pt nanocrystals. As a result, we believe that a significant contribution toward enhanced selectivity must arise from the blocking of unselective Pt metal sites by Co as the second metal, which decreases the extent of C═C hydrogenation, particularly for those smaller Pt sizes. However, this explanation is not comprehensive, since further enhancement in selectivity beyond the 85% limit of undoped large Pt crystals cannot be achieved. There is also a clear promotion effect in boosting selectivity as well as activity upon Co decoration. The apparent selectivity dependent nature of the second metal and the spectacular size-dependent effect clearly suggest another concurrent role of the Co decoration.

It is interesting to observe, from Table 3, the progressive red shift in the $\upsilon_{c=o}$ (linear mode), with decreasing size of Co-decorated Pt nanocrystals. Bearing in mind that the Co atoms are preferentially decorated on the low coordination sites at low surface coverage, the results therefore clearly imply that the exposed Pt atom

TABLE 3. Shift in $\upsilon_{c=o}$ Wavenumber over Different Sizes of Co Decoration on Pt Nanocrystals

Co decorated Pt nanocrystal size (nm)	% selectivity toward unsaturated alcohol	linear peak position (cm^{-1})
4.0	99.7	2047
6.1	99.4	2052
14.6	96.8	2061
17.4	89.4	2063
24.8 (Pt only)	85.3	2060 (literature)

bearing a CO ligand must experience an increasing degree of back-bonding of its d-electrons (increasing δ- on the Pt) to the π* of the CO, when it is placed closer to the Co atoms on smaller size Pt crystals. Examination of the XPS spectra of these samples indeed reveals that there are more significant and progressive shifts in Pt Auger peaks NNN and Co LMM peaks than their core peaks (Co exerts a greater electronic influence to Pt on the outermost electrons and *vice versa*, as reported in PtCo alloy[20]). This is indicative of the local electronic properties of the Pt is influenced by increasing Co atoms content placed in a close proximity to the Pt ensemble. A similar local electronic effect was reported by Janssens *et al.*[21] who calculated that the binding energy shifts on Rh (111), due to the variation of local work function, as a function of the distance from a potassium adsorption site. They observed that the lowering of work function at longer distances depends on the potassium coverage. The catalytic significance of our work is that it represents the differences in the electronic properties that a substrate (α,β-unsaturated aldehyde) experiences at different positions on the surface from the doped Co atoms on the low coordination sites. The δ+ of the deposited Co atoms will attract the carbonyl group aligning the substrate as head-on attack, while the δ- of the neighboring surface Pt atoms destabilizes the adsorption of the C═C bond and thus further enhances selectivity in small crystals. In contrast, the local electronic influence of doped Co atoms cannot cover the entire Pt surface atoms at low coverage in large crystals, hence accounting for the effect of critical size dependence (see models in Figure 5).

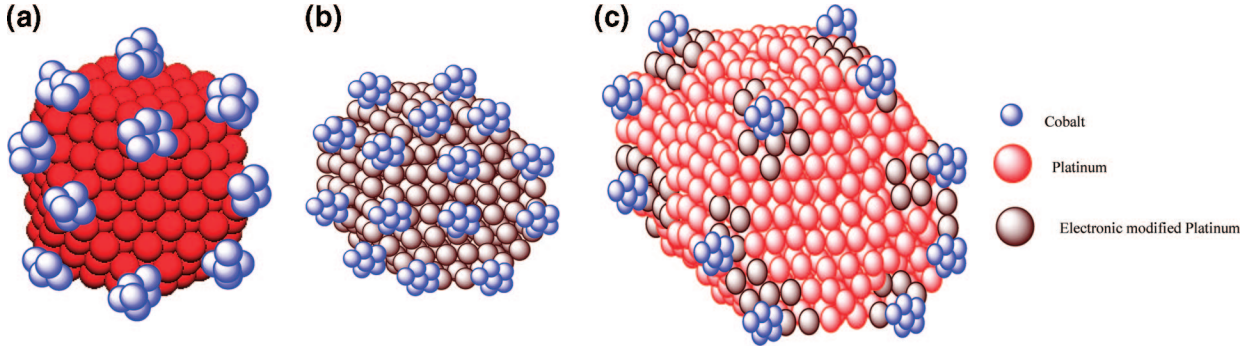

Figure 5. Pictorial models accounting for the critical size effect: (a) model showing Co atoms decorating on corner sites of Pt crystal. (b,c) Models accounting the critical size effect: (b) Co atoms decorated on corners electronically influencing the whole small Pt ensemble-left; (c) some normal Pt sites remained without being influenced by decorated Co atoms in a large Pt ensemble.

It is noted that a smart nanochemistry synthetic method for the preparation of well-defined core−shell bimetallic nanocrystals using preformed noble metal seeds[22] and a shape dependent catalytic activity of platinum nanoparticles have recently been reported.[23] Through engineering of the preformed Pt particles, this technique provides a unique way to totally eliminate such undesirable C═C hydrogenation during the selective hydrogenation of α,β-unsaturated aldehydes by placing the second metal promoter on specific sites and tailoring the size for 100% selectivity. It is worthy noting that conventional catalysts, with poor control in size and unspecific site decoration, are unable to offer such ultrahigh selectivity; they merely average the contributions from individual unoptimized components.

Preliminary results also indicate that our optimized preformed Co-doped Pt can be recycled without support as well as be placed on carbon support; in both cases, its superior activity and selectivity is maintained. On the other hand, one should still be cautious about the long-term stability of the small Co-atoms decoration on the surface as a compromise of activity, selectivity, and stability in relation to catalyst structure/geometry but, for this new type of catalysts, a rational design is allowed.

CONCLUSION

To summarize, nanochemical syntheses have been exploited to atomically decorated preformed Pt nanoparticles with Co of a critical size range that exhibit extraordinarily high selectivities for the carbonyl reduction in α,β-unsaturated aldehydes. The ability to assemble functional catalyst particles, *via* a bottom-up construction approach may enable exploitation of exciting ideas such as catalyst site isolation, differentiation, and optimization or its control access by substrate molecule within a single catalyst particle. This approach could open up a new avenue for preparing new ultraselective and robust catalysts for a wide range of interesting and industrially critical reactions.

METHODS

In a typical Polyol reaction, a solution of platinum(II) acetyl acetonate (99.99%, Aldrich, 0.30 g), 1,2-hexadecanediol (90%, Aldrich, 0.20 g), oleic acid (99+%, Aldrich, 120 μL), and oleylamine (98%, Aldrich, 120 μL) were combined in 10 mL of octylether (99%, Aldrich) and refluxed (with continuous stirring) at 250 °C for 40 min in a three-necked round-bottom flask, under nitrogen. This gave the 4.8 nm Pt nanoparticles. By varying the concentrations of the stabilizers—under the conditions—different sizes of Pt nanoparticles were prepared (see Supporting Information). For the synthesis of Co atom-decorated Pt nanoparticles, separate solutions of cobalt acetyl acetonate, $Co(acac)_2$, (min 97%, Merck, 0.05 g) in 5.0 mL of octylether, combined with 64 μL of oleic acid and 1,2-hexadecanediol (90%, Aldrich, 0.50 g), in octylether were prepared. The solutions were initially distilled at 100 °C for 60 min to remove water. The cobalt acetyl acetonate solution was then injected into the previous colloidal solution, containing platinum nanoparticles, at 200 °C. The nitrogen gas flow was increased as a precautionary measure to maintain the oxygen-free environment, during the injection process. The mixture was then heated to 250 °C and held there for 20 min. The reaction mixture was then allowed to cool to laboratory temperature (~20 °C). The colloidal dispersion was centrifuged to precipitate the nanoparticles and repeatedly washed in ethanol and hexane for at least four times to remove adsorbed solvent molecules, stabilizers, and reducing agents. Variation in Co content on 4.8 nm Pt seeds and syntheses of Co atoms-decorated Pt seeds of different sizes (Co: Pt was kept at 1:1 molar ratio) were performed. The particles were then redispersed into hexane before their direct use or impregnation on carbon support.

The nanoparticles were characterized by transmission electron microscopy (TEM). TEM images were taken by FEI /Philips CM 20. The samples were prepared by placing a drop of colloidal dispersion of nanoparticles in isopropyl alcohol onto a carbon-coated copper grid, followed by naturally evaporating off the solvent. The powder of the nanoparticles was investigated by X-ray powder diffraction (XRD), Siemens D500 X-ray diffractometer with Cu Kα radiation. The surface chemical analyses of Pt and Co were determined by XPS analysis. XPS was performed in a VG Microtec ion pumped XPS system equipped with a nine channel CLAM4 electron energy analyzer. A 200 W Mg X-ray excitation was used. CO adsorption on the surface of nanoparticles was investigated by ATR-IR. The spectra were acquired using a Nicolet 6700 ATR-IR spectrometer with a liquid-nitrogen-cooled MCT detector. A small drop of test sample was placed on smart golden gate-ZeSe/diamond crystal surface and evaporated at room temperature. The spectra were obtained by averaging 512 scans with a resolution of 4 cm^{-1} over the wavenumbers ranging from 650 to 4000 cm^{-1}.

Acknowledgment. We thank David Thompsett of Johnson Matthey Technology Centre (JMTC) of the U.K. for useful discussion and Richard Smith of JMTC, U.K., for the XPS and AES studies.

Supporting Information Available: Material characterization and reaction parameters/size obtained. This material is available free of charge *via* the Internet at http://pubs.acs.org.

REFERENCES AND NOTES

1. Grunes, J.; Zhu, J.; Somorjai, G. A. Catalysis and Nanoscience. *Chem. Commun.* **2003**, 2257–2260.
2. Yeung, C. M. Y.; Yu, K. M. K.; Fu, Q. J.; Thompsett, D.; Petch, M. I.; Tsang, S. C. Engineering Pt in Ceria for a Maximum Metal-Support Interaction in Catalysis. *J. Am. Chem. Soc.* **2005**, *127*, 18010–18011.
3. Gallezot, P.; Richard, D. Selective Hydrogenation Of α,β-Unsaturated Aldehydes. *Catal. Rev. Sci. Eng.* **1998**, *40*, 81–126.
4. Claus, P. Selective Hydrogenation Of α,β-Unsaturated Aldehydes And Other C═O And C═C Containing Compounds. *Top. Catal.* **1998**, *5*, 51–62.
5. Milone, C.; Ingoglia, R.; Schipilliti, L.; Crisafulli, C.; Neri, G.; Galvagno, S. Selective Hydrogenation of α,β-Unsaturated Ketone to α,β-Unsaturated Alcohol on Gold-Supported Iron Oxide Catalysts: Role of the Support. *J. Catal.* **2005**, *236*, 80–85.
6. Galvagno, S.; Capanelli, G.; Neri, G.; Donato, A.; Pietropaolo, R. Hydrogenation of Cinnamaldehyde over Ru/C Catalysts: Effect of Ru Particle Size. *J. Mol. Catal.* **1991**, *64*, 237–246.
7. Yu, K. M. K.; Yeung, C. M. Y.; Thompsett, D.; Tsang, S. C. Aerogel-Coated Metal Nanoparticle Colloids as Novel Entities for the Synthesis of Defined Supported Metal Catalysts. *J Phys. Chem. B* **2003**, *107*, 4515–4526.
8. Pileni, M. P. Nanosized Particles Made in Colloidal Assemblies. *Langmuir* **1997**, *13*, 3266–3276.
9. Sun, S.; Murray, C. B.; Weller, D.; Folks, L.; Moser, V. Monodispersed FePt nanoparticles and Ferromagnetic FePt nanocrystal superlattices. *Science* **2000**, *287*, 1989–1992.

10. Goia, D. V. Preparation and Formation Mechanism of Uniform Metallic Particles in Homogeneous Solutions. *J. Mater. Chem.* **2003**, *14*, 451–458.
11. Delbecq, F.; Sautet, P. Competitive C═C and C═O Adsorption of α,β-Unsaturated Aldehydes on Pt and Pd Surfaces in Relation with the Selectivity of Hydrogenation Reaction: A Theoretical Approach. *J. Catal.* **1995**, *152*, 217.
12. Freund, H. J.; Libuda, J.; Baumer, M.; Risse, T.; Carlsson, A. Clusters, Facets and Edges. Site-Dependent Selective Chemistry on Model Catalysts. *Chem. Rec.* **2003**, *3*, 181–200.
13. Li, H.; Chen, X.; Wang, M.; Xu, V. Selective Hydrogenation of Cinnamaldehyde to Cinnamyl Alcohol over an Ultrafine Co-B Amorphous Alloy Catalyst. *Appl. Catal., A* **2002**, *225*, 117–130.
14. Charles de Ménorval, L.; Chaqroune, A.; Coq, B.; Figueras, F. Characterisation of Mono- and Bi-Metallic Pt Catalysts Using Co FTIR Spectroscopy: Size Effects and Topological Segregation. *J. Chem. Soc., Faraday Trans.* **1997**, *93*, 3715–3720, and references therein.
15. de Caro, D.; Bradley, J. S. Investigation of the Surface Structure of Colloidal Platinum by Infrared Spectroscopy of Adsorbed CO. *New J. Chem.* **1998**, *126*, 7–1273.
16. Manceron, L.; Tremblay, B.; Alikhani, M. E. Vibrational Spectra of PtCO and $Pt(CO)_2$ Isolated in Solid Argon: Trends in Unsaturated Group 10 Metal Carbonyl Molecules. *J. Phys. Chem. A* **2000**, *104*, 3750–3758.
17. Knözinger, H. Metal Clusters and Particles As Catalyst Precursor and Catalysts. In *Cluster Models For Surface And Bulk Phenomena*; Pacchioni, G., Bagus, P. S., Parmigiani, F., Eds.; NATO ASI Series B: Physics; Plenum: New York, 1992; *Vol. 283*, pp 131−149.
18. Attard, G. A.; Gillies, H. C. A.; Jenkins, D. J.; Johnston, P.; Price, M. A.; Watson, D. J.; Wells, P. B. Electrochemical Evaluation of the Morphology and Enantioselectivity of Pt/Graphite. *Appl. Catal., A* **2001**, *222*, 393–405.
19. Attard, G. A.; Griffin, K. G.; Jenkins, D. J.; Johnston, P.; Wells, P. B. Enantioselective Hydrogenation of Ethyl Pyruvate Catalysed by Pt/Graphite: Superior Performance of Sintered Metal Particles. *Catal. Today* **2006**, *114*, 346–352.
20. Lee, Y. S.; Lim, K. Y.; Chung, Y. D.; Kang, H. J.; Wang, C. N. Core Level and Auger Line Shifts in Copt Alloys. *J. Surf. Anal.* **1999**, *6*, 45–49.
21. Janssens, T. V. W.; Wandelt, K.; Niemantsverdriet, J. W. Long and Short Range Effect of Alkali Promoters on Metal Surfaces: K on Rh(111). *Catal. Lett.* **1993**, *19*, 263–272.
22. Habas, S. E.; Lee, H.; Radmilovic, V.; Somorjai, G. A.; Yang, P. Shaping Binary Metal Nanocrystals through Epitaxial Seed Growth. *Nat. Mater.* **2007**, *6*, 602–607.
23. Narayanan, R.; El-Sayed, M. A. Shape-Dependent Catalytic Activity of Platinum Nanoparticles in Colloidal Solution. *Nano Lett.* **2004**, *7*, 1343–1345.